

Continuous Conversion of Rapeseed Oil to Bio-Fuels on 10VNi-10Ce / γ - Al₂O₃ Catalyst

^{1,2}Xigen Huang, ¹Zhiping Le* and ¹Lin Li

¹Department of Chemistry, Nanchang University, Nanchang, 330031, P. R. China.

²Department of Chemistry, Jiangxi Agricultural University, Nanchang 330045, P. R. China.

zple2013915@163.com*

(Received on 1st December 2014, accepted in revised form 6th June 2015)

Summary: Deoxygenation of rapeseed oil over V and Ni supported on Al₂O₃ promoted by Ce was investigated. The supported catalyst was prepared by incipient wetness impregnation method. The obtained catalyst was characterized using techniques of XRD, BET, NH₃-TPD, H₂-TPD and TPR analysis. The results revealed that the catalyst had good thermal stability and three kinds of acidities sites. Compared with sintering, the catalyst deactivation was due to coke deposition. The results of FT-IR, SF-3, GC and GC-MS indicated that reaction temperature is the key factor and that oil velocity is very important factor and that reaction pressure is a less important one in producing bio-fuels. The condition was optimized under such circumstances -- reaction temperature at 450°C, reaction pressure at 3.0MPa, oil velocity at 0.1mL/min and the gas velocity at 30mL/min, respectively. The alkanes content and alkenes content of liquid products are 60.03% and 29.44%, respectively, under the optimized condition. The main products are the hydrocarbon compounds under C₁₈. The results of GC and SF-3 showed that the reaction of decarboxylation and decarbonylation occurred at the same time, and that the oxygen in the oil is mainly removed by the forms of CO and CO₂, and that small part is removed by the form of H₂O. From the results of FT-IR, SF-3 and GC-MS, the generating mechanism of Non- ester renewable diesel was deduced.

Keywords: Bio-fuels, Deoxygenation, 10VNi-10Ce / γ - Al₂O₃ catalyst, Decarboxylation.

Introduction

Global crude oil resources are declining day by day and the quality of crude oil is becoming poorer and poorer every day. The demand of crude oil has been on the increase by 26% every year since 1995 caused by the rapid growth of the world economy [1-3], so the price of the crude oil in the international market in recent years has been soaring. In addition, the environmental problems caused by the extensive use of fossil fuels have been more serious. Seeking and developing renewable energy sources (RES) become even more important to national government. The use of RES is considered to be a solution to the problems of energy lacking and pollution caused by the extensive use of fossil resources in the long-term.

People are paying more and more attention to bio-fuels. Biomass is the only renewable resource containing carbon and can be converted into liquid fuels and chemicals [4, 5]. The conversion of biomass into hydrocarbon is regarded as a carbon neutral process between the chemical conversion (Biomass → hydrocarbon + CO₂) and the photosynthesis (light + CO₂ + H₂O → Biomass), so bio-fuels can be considered to zero emission of CO₂. Compared with fossil fuel, plant contain less of sulfur and nitrogen, so the content of sulfur and nitrogen is less in

bio-fuels, which gives lower emissions of SO₂ and NO_x [6-9].

The conversion of rapeseed oil to bio-fuels was first attempted more than 100 years ago because of the shortage of petroleum, especially in those areas lack of petroleum deposits [10, 11]. The first generation of bio-fuels was called fatty acid methyl ester (FAME) which is liquid bio-fuels that can be produced from a variety of biomass feedstock using suitable conversion technique. Biodiesel production can also be carried out using homogeneous alkali, homogeneous acid and enzyme [12-18]. Direct transformation of rapeseed oil to bio-fuels has been patented by several companies [19-22].

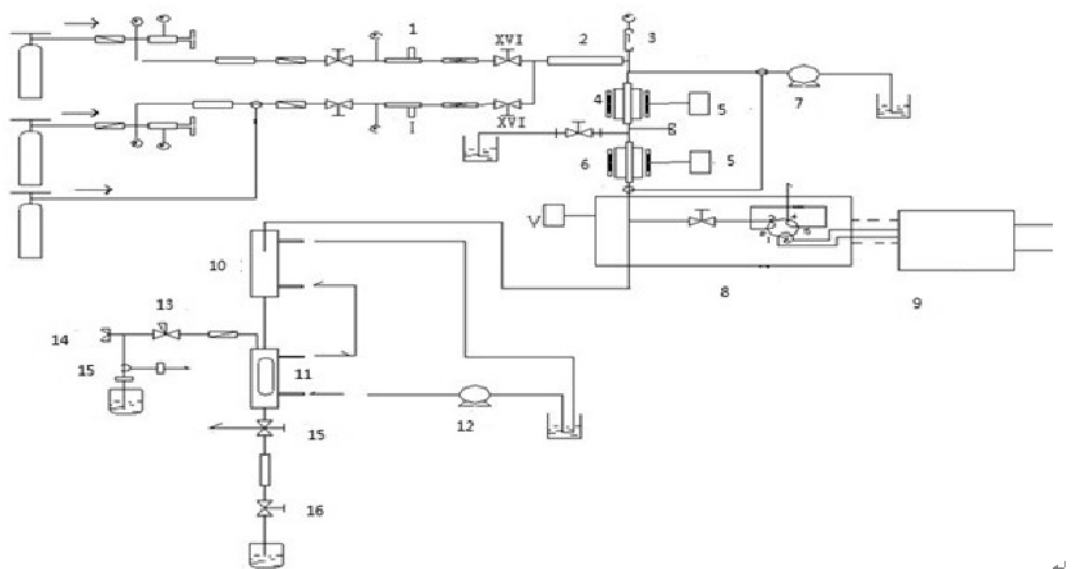
Compared with petroleum-derived fuel, FAME has many physical-chemical disadvantages, such as higher cloud point, higher viscosity, freezing point, pour point and the poor oxidation stability [23-24]. The way of solving these disadvantages is to transform from rapeseed oil to Non- ester renewable diesel (NERD) [25], which is called second generation of bio-fuels. M. Snáře, I. Kubičková, etc [26-28] and Y. Takemura [29] researched the deoxidization of triglycerides to NERD. The deoxidization of fatty acids and their methyl esters

has been studied extensively over Pt/ γ -Al₂O₃ [30], Pd/SBA-15 [31] and Pd/C [32] catalysts. Moreover, the deoxidization of triglycerides can be achieved over these catalysts such as sulfided CoMo, NMo and NiW supported on γ -Al₂O₃ [33] and Ni-Mo/ γ -Al₂O₃/F Catalysts [34]. Masaru Watanab reported ZrO₂, CeO₂ and Y₂O₃ as a solid base catalyst to produce bio-fuels from the waste rapeseed oil by using the Supercritical fluid technique. V₂O₅/ γ - Al₂O₃ had an effective activity in deoxygenation [35-37].

The aim in this paper is to prepare new catalyst for conversion of rapeseed oil to NERD. Effective double metal catalysts were produced by using γ -Al₂O₃ as carrier and V and Ni as activity center, and more effectiveness by using Ce to modify. The condition was optimized on the expediently modified 10VNi-10Ce catalyst under such circumstances -- reaction temperature at 450°C, reaction pressure at 3.0MPa, oil velocity at 0.1mL/min and the gas velocity at 30mL/min, respectively. The alkanes content and alkenes content of liquid products are 60.03% and 29.44%, respectively. The research result of continuous conversion of rapeseed oil to bio-fuels provided a theoretical foundation and scientific basis for solving the problems of energy shortage and greenhouse.

Experimental

Rapeseed oil (industrial grade) with the following mass distribution of fatty acids (purchased from FuLinMen Co. Ltd, Beijing, China) was used as a starting material: palmitic acid: 5.4%, stearic acid:1.87%, oleic acid: 46.04%, linoleic acid:20.36%, linolenic acid:7.98%, eicosanoic acid: 0.63%, eicosenoic acid: 1.75%, erucic acid 15.75%. Conversion of rapeseed oil to bio-fuels was carried out in WFSM-3060 device (Fig. 1). The reactor was loaded prior to the experiments with catalyst diluted by an inert (SiO₂) to ensure sufficient catalyst-bed length and to improve the reaction-heat transfer. A layer of the inert material was placed above the catalyst bed to preheat rapeseed oil and hydrogen and to guarantee a good feed flow distribution prior to entering the catalyst bed. The catalyst was reduced by hydrogen for 2 h at 500°C in situ prior to the experiments. After the reduction, the reactor temperature was decreased to desired temperature under a flow of H₂. The temperature was raised to the desired temperature in all experiments at 10°C/ min. The rapeseed oil and H₂ were mixed by a T-junction.



- | | | | | |
|--------------------|----------------------------|------------------------------|-------------------------------|---------------------------|
| 1. Mass flow meter | 2. Mixer | 3. Relief valve | 4. Carburetor | 5. Temperature controller |
| 6. Reactor | 7. Trace injection pump | 8. Thermotank | 9. Chromatographic instrument | |
| 10. Condensator | 11. Gas - liquid separator | 12. Refrigerated medium pump | | |
| 13. Pressure value | 14. Offline sampling port | 15. Three-way valve | 16. Switch valve | |

Fig. 1: WFSM-3060 patterns of the reaction device.

Catalyst Preparation

Prior to adding nitrate, the γ - Al_2O_3 support pellets were calcined in air at 773 K for 5 h in order to stabilize the surface area. Aqueous solution of nickel nitrate, ammonium metavanadate (NH_4VO_3), oxalic acid ($\text{C}_2\text{H}_2\text{O}_4$) and cerium nitrate were deposited into the support of γ - Al_2O_3 by wetness impregnation. The immobilization loading of V-Ni bimetallic catalyst was 10wt% and 10VNi-10Ce/ γ - Al_2O_3 catalyst was obtained by adding desired amount of cerium nitrate into the mixture solution of nickel nitrate and NH_4VO_3 before drying in oven.

Characterization Method

The textural characteristics of the support and catalysts were analyzed by N_2 physisorption method. N_2 adsorption and desorption isotherms were performed at 77 K on Micromeritics ASAP2020C equipment. The samples were outgassed in vacuum ($\approx 1\ \mu\text{m Hg}$) at 573 K for 3 h before the measurement. The pore diameter and pore volume were calculated from the analysis of desorption branch of the isotherm by the Barrett-Joyner-Halenda method. Temperature programmed reduction (TPR) measurements were performed with a Chemisorb 2750 instrument. The catalyst samples were purged with argon at 150°C for 30 min and cooled to 20°C, then heated to 840°C at a rate of 10°C min^{-1} while flowing a 5vol% H_2/Ar (50 $\text{cm}^3\ \text{min}^{-1}$) through the sample. The consumption of hydrogen was monitored by a thermal conductivity detector (TCD). Deposited coke was measured by temperature programmed combustion, performed on a thermogravimetric TGA/SDTA851 device. Temperature programmed desorption (TPD) measurements were performed with a Chemisorb2920 instrument. The catalyst samples were purged with argon at 150°C for 30 min and cooled to 50°C before the measurement of H_2 or NH_3 adsorption.

Gas Products Analysis

The gas products were online analyzed by GC. GC equipped with a thermal conductivity detector and carbon molecular sieve column TDX-01 (2.0 m, 2.0mm), were used to analyze the contents of CO and CO_2 at a constant temperature of column 190°C, current 110mA and detector 160°C, respectively.

Liquid Products Analysis of FT-IR

The FT-IR spectra of the liquid product

samples were recorded by a Nicolet 5700 27 Infrared Spectrophotometer in 4000-400 cm^{-1} with KBr pellet sample.

Liquid Products Analysis of GC-MS

GC-MS analysis using an Agilent 7890A GC (HP-5 column, 30 m \times 0.25 mm \times 0.25 μm) coupled to an Agilent 5975C Inert MSD with a quadruplicate axis detector. Liquid products were diluted 1:1 in cyclohexane and 0.2 μL of the diluted sample was injected onto a HP-5 column. Helium was used as the carrier gas at velocity rate with 54mL/min and split ratio was 50:1.

Trace Water Content Measurement of Liquid Products

Karl-Fisher coulometric titration method has been adopted to determine trace water content measurement to different substances. SF-3 (made in Zibo Instrument Co., Ltd, China) trace water content meter has successfully adopted this method.

Result and Discussion

BET

BET has been used to analyze the catalysts before used and has been used. The results were shown in Fig. 2 and Table-1. It can be seen from Table-1 that the surface areas and the pore volume have a very slight decrease for the catalyst of fresh and has been multiple used. The result indicated that the 10VNi-10Ce/ γ - Al_2O_3 catalyst can keep structure stability in this reaction. Comparatively speaking, the catalyst deactivation was due to coke deposition rather than sintering.

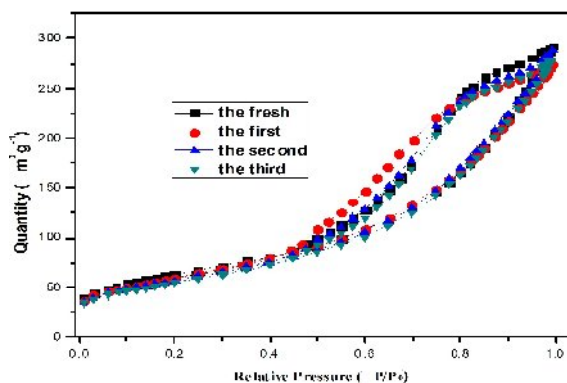


Fig. 2: BET patterns of the fresh and used catalyst.

Table-1: BET parameter of fresh and the used catalysts.

	Fresh	The first	the second	the third
BET Surface Area(m ³ /g)	225.39	212.12	206.35	198.42
Single point adsorption total pore volume of pores(cm ³ /g)	0.4272	0.4142	0.4137	0.4059
BJH Adsorption cumulative volume of pores(cm ³ /g)	0.4639	0.4627	0.45878	0.4385
BJH Desorption cumulative volume of pores(cm ³ /g)	0.458	0.4547	0.45359	0.4354
Adsorption average pore width(nm)	7.5814	7.6151	7.84699	8.182
BJH Adsorption average pore diameter(nm)	7.8335	7.7189	7.76705	7.6291
BJH Desorption average pore diameter(nm)	6.2317	6.2572	6.254	6.3455

TPR

The TPR result of the catalyst is shown in Fig. 3. It can be found from Fig. 3 that the reduction peak at 358 °C for Ni20 catalyst is attributed to the reduction of Ni²⁺ in the NiO phase, and the second peak at 437°C is assigned to the reduction of Ni²⁺ in NiAl₂O₄. The reduction peak at 357°C for V20 catalyst is assigned to the reduction of V⁵⁺ → V³⁺. In Fig. 3, catalyst 10V10Ni and 10VNi-10Ce have two reduction peaks. The reduction peaks of 10VNi catalyst are at 400°C and 500°C. Compared with 10VNi catalyst, the reduction temperature peaks of 10VNi-10Ce catalyst shifted to higher temperature (460°C and 560°C). The result implies the synergic effect produced in the process of catalyst preparation among cerium, nickel and vanadium species. The results reveal that cerium plays an important role in the reduced process.

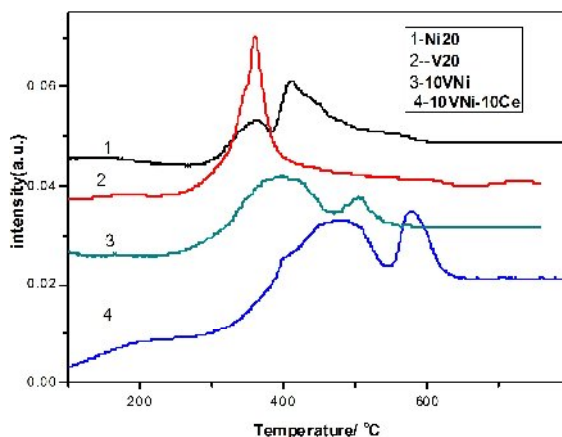
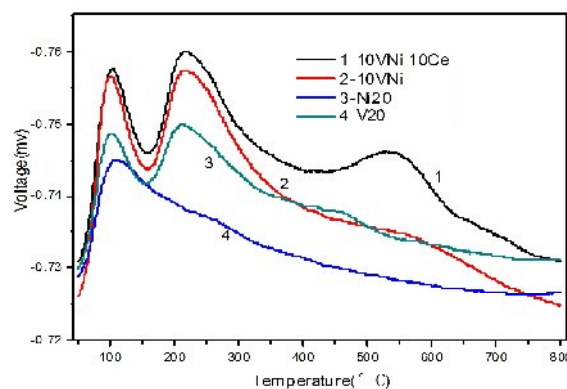


Fig. 3: TPR patterns of the different catalysts.

NH₃-TPD

To characterize the total acid sites on catalysts, NH₃-TPD was carried out using a Chemisorb2920. The results are shown in Fig. 4. For all catalysts an intense desorption peak is observed at 120°C, which can be attributed to weakly absorbed NH₃. For V20 and 10VNi catalysts show similar NH₃ desorption curves with an intense peak at 220 °C.

Moreover, a broad ammonia desorption peak occurs over the whole desorption temperature range. The peak at 220 °C could be assigned to ammonia adsorbed on the acid sites including weakly and strongly bound NH₃ species. The 10VNi-10Ce catalyst shows higher ammonia desorption peak area at high temperature (550°C), which is assigned to the ammonia strongly adsorbed on acid sites. The results of NH₃-TPD indicate that the catalyst modified by Ce (10VNi-10Ce) had the largest number of strong acid sites. The strong acid site is beneficial to the catalyst activity of the hydrogenation reaction and the deoxidization reaction [36-37].

Fig. 4: NH₃-TPD profile of the different catalysts.

H₂-TPD

The result of H₂-TPD is given in Fig. 5. The H₂-TPD profile in Fig. 5 shows that two peaks of adsorbed sites at around 120°C and 220°C can be seen in all kinds of catalysts. However, there were different hydrogen desorption curves over 400°C for different catalysts. For Ni20 and V20 catalyst, the shoulder desorption peaks were centered at 450°C. For 10VNi and 10VNi-10Ce catalysts, the high temperature desorption peaks were centered at 550°C. The result of H₂-TPD also showed that the 10VNi-10Ce catalyst had higher desorption peak area at the high temperature than other catalysts. The higher desorption temperature makes desorption of

reaction H₂ harder, which is beneficial to the hydrogenation reaction. The strong adsorbed site is beneficial to the catalyst activity of the hydrogenation reaction [36-37].

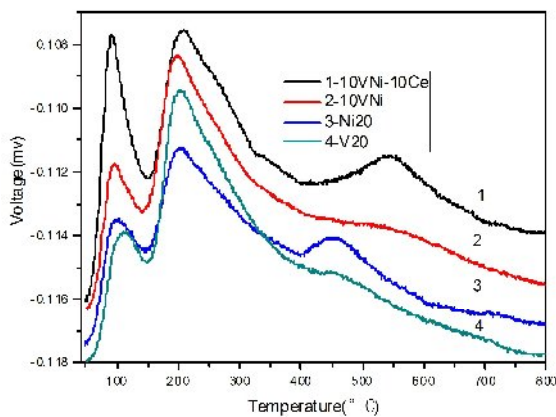


Fig. 5: H₂-TPD patterns of the different catalysts.

Selection of the Optimized Condition

All sorts of bio-fuels productions were carried out by WFSM-3060 device. The gas products were collected and online analyzed by GC in order. The crude oil and the liquid products were analyzed by FT-IR, SF-3 and GC-MS.

Effect of Different Reaction Temperature

The experiments of different reaction temperatures were performed respectively at 470°C, 450°C, 430°C, 410°C, 390°C and 360°C. The products of six reaction temperatures were obtained at reaction pressure of 2.5MPa, the crude oil flow rate of 0.1mL/min and the H₂ flow rate of 25mL/min. Liquid yield, gas yield, H₂O content, coke yield and the distribution of liquid hydrocarbons were described and shown in Table-2. As Table-2 displays, when reaction temperatures decreased from 470°C to 360°C, liquid yield was obtained from 85.95%, 86.84%, 87.08%, 87.76%, 87.93% to 88.13%; H₂O content, from 0.037%, 0.058%, 0.059%, 0.106%, 0.120% to 0.135%; Coke yield, from 1.11%, 1.27%, 1.30%, 1.48%, 1.75% to 2.03%; oxygenated compound content, from 0.86%, 5.90%, 6.14%, 7.63%, 7.04% to 8.50%; the alkanes content of liquid products, from 38.42%, 43.37%, 46.69%, 42.37%, 37.33% to 38.1%; alkenes content of liquid products, from 40.81%, 42.14%, 37.83%, 42.14%, 41.63% to 40.09%. Liquid yield of the products of different

reaction temperatures have tiny aggrandizement.

Table-2: The analytical result of conversion of triglycerides to bio-fuels at different reaction temperatures.

	470°	450°	430°	410°	390°	360°
	C	C	C	C	C	C
Liquid yield%	85.95	86.84	87.08	87.76	87.93	88.13
Gas%	12.9	11.84	11.56	10.65	10.2	9.7
Coke%	1.11	1.27	1.3	1.48	1.75	2.03
H ₂ O%	0.037	0.058	0.059	0.106	0.12	0.135
Composition of the liquid product						
alkanes	38.42	43.37	46.69	42.37	37.33	38.1
alkenes	40.81	42.14	37.83	42.14	41.63	40.09
Oxygenated compounds	0.86	5.9	6.14	7.63	7.04	8.5
cyclic compounds	8.01	4.84	4.76	3.75	6.31	6.61
aromatics	11.9	3.16	4.47	3.16	7.15	6.66
C ₈ -C ₁₀ wt%	8.03	2.21	3.4	2.21	4.79	4.94
C ₁₁ -C ₁₈ wt%	73.95	85.08	81.49	83.48	78.62	73.11
C ₁₈₊ wt %	18.02	12.12	15.0	13.36	16.05	21.91

Total content of alkanes and alkenes is lower and the content of oxygenated compound is higher in the 410°C, 390°C and 360°C products than the 450°C and 430°C products; the products produced at 410°C, 390°C and 360°C had poor liquidity. The effect of thermal cracking and catalytic cracking decreased because of the drop at reaction temperature, and the 410°C, 390°C and 360°C products have higher coke deposition and the higher content of oxygenated compound. Compared with the other products, total content of alkanes and alkenes is higher in the 450°C and 430°C product, the total content of oxygenated compound, aromatic hydrocarbon and cyclic compounds are lower. The liquid products are mostly hydrocarbon compounds under C₁₈. Although the content of oxygenated compound in the 470°C product was the lowest in all products, liquid yield and total content of alkanes and alkenes were lower than the products produced at 450°C and 430°C. Moreover, gas yield and total content of aromatic hydrocarbon and cyclic compound in the 470°C products were higher than the 450°C and 430°C products. The technique of 450°C and 430°C are better than the 470°C technique. The liquid products produced at 450°C had the high content of alkanes and alkenes and the low content of oxygenated compounds and coke yield than the liquid product produced at 430°C. The optimized reaction temperature is 450°C.

Coke yield of different reaction temperatures increased more than twice, Oxygenated compound content and H₂O content increased more than four times, which show that reaction temperature is a very key factor in producing bio-fuels.

The molar ratio of CO and CO₂ are listed in Table-3 under various times. It can be seen from Table-3, the proportional relationship between CO and CO₂ is changing with time. The molar ratio of CO₂/CO increased firstly and then decreased as the reaction progresses. But the molar ratio of CO₂/CO is more than twice in most cases, and the molar ratio of CO₂/CO change at about 0.4021~41.02. The result of GC online shows that the reaction of decarboxylation and decarbonylation occur at the same time and decarboxylation reaction was the main reaction. Analytical result of GC gas online and H₂O test indicate that the most products of the oxygen in the crude oil were CO and CO₂, and the tiny product of the oxygen was H₂O.

Table-3: The GC analytical result of the conversion of triglycerides to bio-fuels at different reaction temperatures.

No.	470°C	450°C	430°C	410°C	390°C	360°C
	CO ₂ /CO					
1	1.692	8.772	0.8312	1.123	0.4021	0.8067
2	6.468	8.356	0.8815	1.877	0.8815	0.8815
3	13.62	14.42	3.439	2.503	1.692	3.617
4	9.56	6.934	6.468	2.858	2.089	4.173
5	12.46	7.839	10.24	8.862	3.617	6.468
6	41.02	5.663	14.08	9.537	5.812	4.266
7	10.51	3.221	10.29	17.21	6.468	2.503
8	5.812	2.694	7.547	10.29	5.053	1.656
9	5.12	1.628	6.133	8.355	1.628	1.628
10	4.75	2.694	3.259	7.104	2.503	1.458

It can be seen from Fig. 6, each FT-IR spectrum was normalized by the intensity of the absorption band centered at 2930 cm⁻¹(the strongest band) in all kinds of the products and the crude oil. The C=O bond stretch was observed in the range 1600-1800 cm⁻¹. Compared with FT-IR graph of the crude oil, the intension of the C=O bond stretch in the 1740 ~ 1750cm⁻¹ almost disappeared in the 410°C, 430°C, 450°C and 470°C liquid products while the carbonyl absorption peak of 1705 ~ 1720cm⁻¹ exists. The carbonyl absorption peak is weak and decreasing when the reaction temperature was raised from 360°C to 470°C. The carbonyl absorption peak of 1705 ~ 1720cm⁻¹ disappeared when the reaction temperature was 450°C. That shows that ester bond cleavage occurred and the products produced at 450°C have small amount of ketones compound. It can be seen from Fig. 6 that the intensity of the absorption peak in the area of 1740 ~ 1750cm⁻¹ is strong while the intensity of the absorption peak in the area of 3340 ~ 3320 is weak in the 360°C and 390°C products. That shows that the products have large amount of ketone and tiny fatty acids derivatives containing oxygen. When reaction temperature increased, the deoxygenated effect also

increased. The results of FT-IR and the GC-MS data analysis indicate that the reaction temperature is a very key factor in producing bio-fuels.

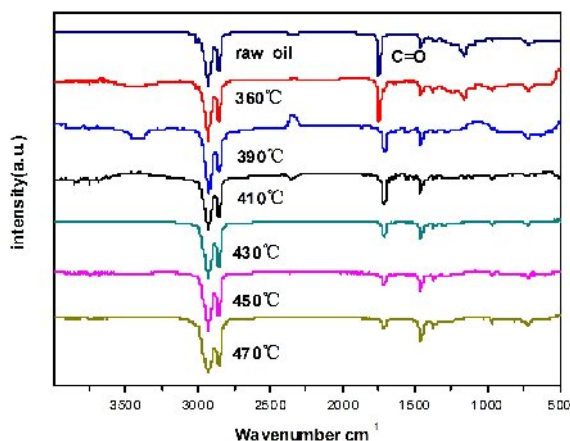


Fig. 6: FT-IR spectra of the liquid products of different reaction temperatures.

Effect of Different Gas Flow Rates

The tests of several carrier gas flow rate were performed at carrier gas flow rate from 40mL/min, 35mL/min, 30mL/min, 25mL/min, 20mL/min and 15mL/min, respectively. The products of six various H₂ flow rates were obtained at reaction pressure of 2.5MPa, reaction temperature of 450°C and the oil flow rate of 0.10mL/min. Liquid yield, gas yield, H₂O content, coke yield and distribution of liquid hydrocarbons were described and shown in Table-4. Compared with the reaction temperature, the change of liquid yield, H₂O content, the total content of the alkanets and alkenes and coke rate is not large increase, which shows that H₂ velocity is a secondary factor in producing bio-fuels.

Table-4: The analytical result of the conversion of triglycerides to bio-fuels at different gas flow rates (gas flow rate: mL/min).

	40	35	30	25	20	15
Liquid yield%	86.55	86.51	86.9	86.84	85.51	85.89
Gas%	11.92	12.03	11.81	11.84	13.13	12.61
Coke%	1.49	1.42	1.22	1.27	1.3	1.42
H ₂ O%	0.035	0.036	0.073	0.058	0.059	0.081
Composition of the liquid product						
alkanes	35.58	41.26	45.35	43.37	36.39	31.44
alkenes	46.2	44.49	40.64	42.14	48.22	51.83
Oxygenated compound	8.7	4.99	5.77	5.9	6.16	7.1
cyclic compounds	6.53	6.14	4.65	4.84	4.95	7.9
aromatics	2.62	2.8	2.1	3.16	1.44	1.54
C ₉ -C ₁₀ wt%	6.04	4.64	5.68	2.21	9.39	5.71
C ₁₁ -C ₁₈ wt%	80.72	77.69	79.59	85.08	75.22	84.53
C ₁₈ ⁺ wt %	12.87	17.35	13.24	12.12	12.55	9.9
Total, wt%	99.63	99.68	98.51	99.41	97.16	99.81

It can be seen from Fig. 7, all kinds of FT-IR spectrum were normalized by the strongest intensity of the absorption band centered at 2930 cm^{-1} . Compared with FT-IR graph of the crude oil, all liquid products have no $1740 \sim 1750\text{ cm}^{-1}$ peak, but the carbonyl absorption peak of $1705 \sim 1720\text{ cm}^{-1}$ exists and the carbonyl absorption peak is weak. That shows that the products have small amount of ketone compound containing oxygen. The result of FT-IR spectra shows that the deoxidization of the crude oil was efficiently performed in various H_2 flow rates.

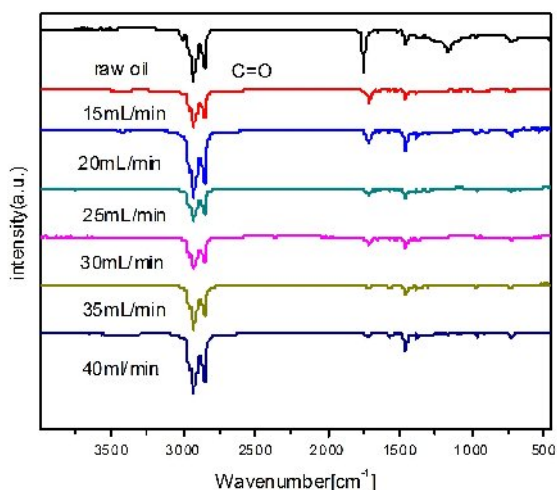


Fig. 7: FT-IR spectra of the liquid products of different gas flow rates.

According to the data of GC-MS, the content of alkanes is the highest in the 30 mL/min liquid product, and the content of coke yield and oxygenated compound are lower than other products of several H_2 flow rate. The main products are hydrocarbon compounds under C_{18} . Moreover, odd carbon hydrocarbons with C_{15} and C_{17} are the main compounds. The good technique is that reaction gas flow rate is 30 mL/min. The crude oil and middle products' stay time became shorter when H_2 flow rate increased in the hydrogen condition. The effect of decarboxylation and decarbonylation reaction would not be good. The total content of alkanes and alkenes became lower in the 40 mL/min liquid product.

The molar ratio of CO and CO_2 is listed in Table-5 under various conditions. It can be seen from Table-5 that CO and CO_2 are simultaneously generated and the proportional relationship between CO and CO_2 is changing with time. The molar ratio CO_2/CO increased firstly and then decreased as the reaction progresses. But the molar ratio of CO_2/CO

is more than twice in most cases, and the molar ratio of CO_2/CO change at about $0.5427 \sim 35.62$. In the 40 mL/min, 35 mL/min and 30 mL/min gas flow rate, the molar ratio of CO_2/CO changed more than ten times for 4 ~ 7 times. The result of GC online shows that the reactions of decarboxylation and decarbonylation occur at the same time and decarboxylation reaction was the main reaction.

Table-5: The analytical result of the conversion of triglycerides to bio-fuels at different gas flow rates.

No.	40	35	30	25	20	15
	CO_2/CO	CO_2/CO	CO_2/CO	CO_2/CO	CO_2/CO	CO_2/CO
1	5.663	10.96	5.053	8.775	0.5427	1.224
2	9.838	10.77	8.114	8.355	2.233	2.342
3	10.1	18.6	7.644	14.43	5.684	3.258
4	10.71	13.99	15.61	10.24	10.75	5.663
5	9.613	20.1	19.29	6.937	9.822	3.513
6	20.55	29.66	26.85	7.842	10.242	2.767
7	13.27	35.62	19.22	5.662	10.28	1.771
8	8.289	28.94	23.37	3.615	7.545	1.656
9	7.304	23.99	7.477	3.221	6.135	1.629
10	3.513	11.45	8.959	2.694	3.221	1.525

The results of GC online and trace water test shows that the most oxygen of the crude oil were rejected by the forms of CO and CO_2 , and a small quantity of the oxygen was rejected by the form of H_2O .

Effect of Different Oil Flow Rate

The experiments of several crude oil flow rates were performed at the crude oil flow rate with 0.06 mL/min, 0.08 mL/min, 0.10 mL/min, 0.12 mL/min, 0.14 mL/min and 0.16 mL/min, respectively. The products of six various crude oil flow rates were obtained at reaction pressure of 2.5MPa, reaction temperature of $450\text{ }^\circ\text{C}$ and the H_2 flow rate of 25 mL/min. Liquid yield, gas yield, H_2O content, coke yield and distribution of liquid hydrocarbons were described in Table-6. When the crude oil flow rate increased from 0.06 mL/min to 0.16 mL/min, liquid yield was consequently obtained from 85.31%, 86.12%, 86.84%, 88.74%, 89.04% to 89.81%; H_2O content, from 0.058%, 0.058%, 0.058%, 0.082%, 0.087% to 0.097%; coke deposition rate, from 1.05%, 1.07%, 1.27%, 1.39%, 2.16% to 2.24%; oxygenated compounds content, from 1.18%, 2.27%, 5.90%, 6.28%, 7.17% to 9.10%. Although the change of the liquid yield and H_2O content is small, the change of oxygenated compound content and coke yield increased more than twice, which shows that oil velocity is a very important factor in bio-fuels producing.

Table-6: The analytical result of conversion of triglycerides to bio-fuels at different oil speeds.

	0.06	0.08	0.1	0.12	0.14	0.16
Liquid yield%	85.31	86.12	86.84	88.74	89.04	89.81
Gas%	13.58	12.75	11.84	9.79	8.71	7.85
Coke%	1.05	1.07	1.27	1.39	2.16	2.24
H ₂ O%	0.058	0.058	0.058	0.082	0.087	0.097
Composition of the liquid product						
alkanes	43.9	40.63	43.37	37.22	26.52	27.81
alkenes	36.62	43.64	42.14	44.06	46.73	45.91
Oxygenated compound	1.18	2.27	5.9	6.28	7.17	9.1
cyclic compounds	8.03	6.27	4.84	6.29	8.4	7.59
aromatics	8.79	6.24	3.16	6.01	9.15	9.02
C ₉ -C ₁₀ wt%	7.79	5.75	2.21	3.6	9.2	6.71
C ₁₁ -C ₁₈ wt%	73.9	82.67	85.08	79.26	73.85	80.36
C ₁₈ ⁺ wt %	16.83	10.63	12.12	17	14.92	12.36
Total, wt%	98.52	99.05	99.41	99.86	97.97	99.43

According to the data of GC-MS, the crude oil flow rate were increased from 0.06 mL/min to 0.16mL/min, oxygenated compound content of different liquid products changed from 1.18%, 2.27%, 5.90%, 6.28%, 7.17% to 9.10%; alkanes content of liquid products, from 43.90%, 40.63%, 43.37%, 37.22%, 26.52% to 27.81%; alkenes content, from 36.62%, 43.64%, 42.14%, 44.06%, 46.73% to 45.91%.

Compared with the other oil speed products, the content of oxygenated compounds is higher in the liquid products produced at 0.12mL/min, 0.14mL/min and 0.16mL/min, which had poor liquidity. From the total content of alkanes and alkenes, the liquid products produced at 0.06mL/min, 0.08mL/min and 0.10mL/min oil speeds are higher than the liquid products produced at 0.12mL/min, 0.14mL/min and 0.16mL/min, and the total content of alkanets and alkenes is the highest in the liquid products produced at 0.10mL/min oil speed. The main products are the hydrocarbon compounds under C₁₈, and most alkanes and alkenes are hydrocarbons with C₁₁~C₁₈, moreover, odd carbon hydrocarbons with C₁₅ and C₁₇ are the main compounds. What's more, the aromatics content in the liquid product produced at 0.06mL/min oil speed is higher than the liquid product produced at oil speed of 0.10mL/min. From the total content of alkanets and alkenes and the LHSV and economic benefits, the technique at 0.10mL/min oil speed is better than the technique at 0.06mL/min oil speed.

It can be seen from Fig. 8, each FT-IR spectrum was normalized by the intensity of the absorption band centered at 2930 cm⁻¹(the strongest band, CH₂ stretching) in all kinds of liquid products. Compared with FT- IR graph of the crude oil, all cracking products almost have no 1740 ~ 1750cm⁻¹ peak, but the carbonyl absorption peak of 1705 ~

1720cm⁻¹ exists, which have small amount of ketone compound. The intensity of the absorption peak decreased when the oil velocity reduced. The peak intensity of C=O almost disappeared in the liquid product produced at 0.1mL/min oil velocity. The FT-IR result shows that the effect of the deoxidization was very efficient at the crude oil velocity of 0.1mL/min.

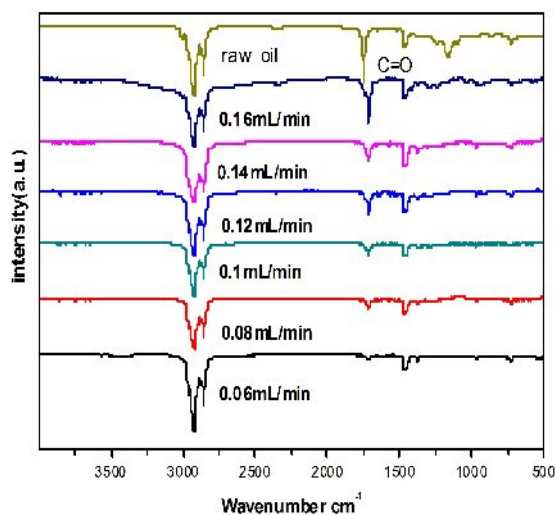


Fig. 8: FT-IR spectra of the liquid products of different oil flow rates.

The molar ratio of CO and CO₂ are listed in Table-7 under various conditions. It can be seen from Table-7, the proportional relationship of CO and CO₂ is changing with the time. The molar ratio of CO₂/CO increased firstly and then decreased as the reaction progresses. But the molar ratio of CO₂/CO is more than twice in most cases, and the molar ratio of CO₂/CO change at about 0.8413 ~ 33.6. The molar ratio of CO₂/CO may change more than five times in the middle period (for 3 ~7 times).

Table-7: The GC result of the conversion of triglycerides to bio-fuels at different oil speeds.

	0.06	0.08	0.1	0.12	0.14	0.16
	CO ₂ /CO					
1	1.666	0.8413	8.775	3.941	6.133	3.156
2	8.699	3.1563	8.3545	10.4	7.54	5.662
3	9.101	5.662	14.43	16.39	9.091	7.104
4	9.255	7.432	10.24	22.09	10.29	8.355
5	8.233	10.24	6.937	24.97	17.21	10.29
6	7.382	10.29	7.842	33.6	24.25	17.21
7	6.716	7.104	5.662	16.45	21.19	9.091
8	6.353	5.053	3.615	14.08	17.2	10.29
9	5.9444	4.65	3.221	7.8417	10.15	7.842
10	5.349	3.221	2.694	7.156	6.133	6.133

Analytical result of GC online and trace H₂O test shows that the most products of the oxygen were CO and CO₂, and the minor products of the oxygen was H₂O.

Effect of Different Reaction Pressure

The experiments of several different pressures were performed from 3.5MPa, 3.0MPa, 2.5MPa, 2.0MPa, 1.5MPa to 1.0MPa. The products of six various different pressures were obtained at the crude oil flow rate of 0.1mL/min, reaction temperature of 450°C and the H₂ flow rate of 25 mL/min. The products in all sorts of different conditions were marked in order as G36, G35, G34, G33, G32 and G31, respectively. Liquid yield, gas yield, H₂O content, coke yield and the distribution of liquid hydrocarbons were described as shown in Table-8. As Table-8 displays, when reaction pressure of the experiment decreased from 3.5MPa to 1.0 MPa, liquid yield was obtained from 86.51%, 86.67%, 86.84%, 86.63%, 86.71% to 86.30%; H₂O content, from 0.035%, 0.098%, 0.058%, 0.057%, 0.055% to 0.075%; coke yield, from 1.19%, 1.16%, 1.27%, 1.26%, 1.33% to 1.42%; oxygenated compound content, from 2.97%, 3.06%, 5.90%, 6.00%, 5.97% to 6.37%; alkanes content of liquid products, from 46.35%, 59.92%, 43.37%, 45.36%, 56.51% to 31.08%; alkenes content of liquid products, from 29.17%, 29.04%, 42.14%, 35.62%, 27.44% to 43.15%. The change of liquid yield, H₂O content and coke yield is not on large increase, but the change of oxygenated compound content increases more than twice.

It can be seen from FT-IR Fig. 9, each FT-IR spectrum was normalized by the intensity of the absorption band centered at 2930 cm⁻¹(the strongest band). Compared with the FT- IR graph of the crude oil, all kinds of products almost have no 1740 ~ 1750cm⁻¹ peak, while the carbonyl absorption peak of 1705 ~ 1720cm⁻¹ exists and the intensity of the

absorption peak is weak, which shows that the products have small amount of ketone compounds. It can be seen from Fig. 9 that the peak intensity of C=O bond of liquid products reduced as the following order: G36≥ G35≥ G34> G33> G32> G31 in the range 1705 ~ 1720 cm⁻¹. The FT-IR result shows that the effect of the deoxidization was very efficient at the 2.5MPa, 3.0MPa and 3.5MPa reaction pressures.

Table-8: The analytical result of conversion of triglycerides to bio-fuels at different reaction pressures (unit: MPa).

	3.5	3	2.5	2	1.5	1
Liquid yield%	86.51	86.67	86.84	86.63	86.71	86.3
Gas%	12.26	12.07	11.84	12.05	11.9	12.2
Coke%	1.19	1.16	1.27	1.26	1.33	1.42
H ₂ O%	0.035	0.098	0.058	0.057	0.055	0.075
Composition of the liquid product						
alkanes	46.35	59.92	43.37	45.36	56.51	31.08
alkenes	29.17	29.04	42.14	35.62	27.44	43.15
Oxygenated compounds	2.97	3.06	5.9	6	5.97	6.37
cyclic compounds	10.2	4	4.84	6.3	7.08	7.8
aromatics	9.68	3.21	3.16	6.64	1.02	9.65
C ₉ -C ₁₀ wt%	8.01	5.63	2.21	5.82	8.15	12.01
C ₁₁ -C ₁₈ wt%	69.04	75.95	85.08	79.98	74.28	75.8
C ₁₈ wt %	21.32	17.65	12.12	14.12	15.59	10.24
Total, wt%	98.37	99.23	99.41	99.92	98.02	98.05

Table-9: The GC result of the conversion of oil to bio-fuels at different pressures.

	3.5	3	2.5	2	1.5	1
No.	CO ₂ /CO					
1	5.337	3.389	8.772	7.839	0.6015	5.155
2	8.248	5.817	8.356	10.89	5.134	7.644
3	10.28	7.644	14.42	11.92	11.61	15.61
4	19.29	15.61	6.934	19.52	13.45	19.29
5	26.85	19.29	7.839	27.77	22.49	25.05
6	35.99	26.85	5.663	34.45	12.69	19.22
7	23.37	35.86	3.221	26.42	15.63	13.17
8	13.43	23.37	2.694	18.23	15.29	10.28
9	13.17	13.43	1.628	10.94	10.76	7.839
10	7.545	8.959	2.694	5.053	7.792	3.258

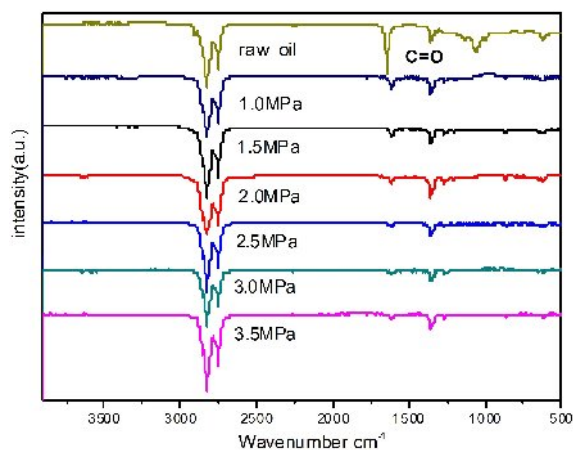


Fig. 9: FT-IR spectra of the liquid products of different reaction pressures.

As Table-8 displays, the content of alkanes, oxygenated compound content, and total content of alkanes and alkenes of the product produced at 3.0MPa were 59.92%, 3.06% and 88.96%. The content of alkanes and total content of alkanes and alkenes in the product of G35 (3.0MPa) were higher than other reaction pressure products. The main products are hydrocarbon compounds under C₁₈ and the molar ratio of the diesel oil boiling range target fraction was relatively high (69.04-85.08%). Moreover, odd carbon products with C₁₅ and C₁₇ are the main compounds. The optimized condition is that reaction pressure is 3.0MPa under the same LHSV and reaction temperature.

The molar ratio of CO and CO₂ are listed in Table-9 under various conditions. It can be seen from Table-9, the molar ratio between CO and CO₂ is changing with the time. The molar ratio of CO/CO₂ increased firstly and then decreased as the reaction progresses. But the molar ratio of CO₂/CO is more than twice in most cases, and the molar ratio of CO₂/CO change at about 0.6015~35.99. The molar ratio of CO₂/CO changed more than five times for 2~6 times. The result of GC online shows that the reactions of decarboxylation and decarbonylation occur at the same time and decarboxylation reaction was the main reaction. Analytical result of GC online and trace H₂O test shows that the most oxygen in the crude oil were rejected by the forms of CO and CO₂, and the minor oxygen was removed by the form of H₂O.

The Optimized Technology

The technique was optimized at reaction temperature of 450°C, reaction pressure of 3.0 MPa, the oil flow rate of 0.1 mL/min and the gas flow rate of 30 mL/min. The liquid product of optimized conditions was marked as G37. The liquid product was analyzed by FT - IR, GC-MS and SF-3, and the gas product was analyzed by GC online. The catalyst was analyzed by BET. The result of GC online shows that the reaction of decarboxylation and decarbonylation occur at the same time and the decarboxylation reaction is the main reaction. The molar ratio of CO₂/CO may change about 5.33~26.50. The gas yield and the liquid yield of optimized conditions were 11.54 wt % and 86.68 wt%; oxygenated product content, H₂O content and coke yield were 3.04 wt%, 0.063 wt% and 1.15 wt%. The alkanes and alkenes content of liquid products were 60.03% and 29.44%, respectively. Compound distribution in the liquid product analyzed by GC-MS was showed in Table-10. The main products are the

hydrocarbon compounds under C₁₈.

Stability and Activity of Catalyst

The stability of 10VNi-10Ce catalyst was performed by WFSM-3060 device at reaction temperature of 450°C, reaction pressure of 3.0 MPa, the oil flow rate of 0.1 mL/min and the gas flow rate of 30 mL/min. The used catalyst was calcined at 600°C for 6 h to remove carbon residue in the muffle stove. Liquid hydrocarbon yields, H₂O content, oxygenated product yield and coke yields were described and shown in Table-11. Liquid hydrocarbon yields and H₂O content have little diversification. Liquid product yield were reduced from 86.68%, 86.63%, 86.48% to 86.19%; H₂O content, from 0.063%, 0.068%, 0.072% to 0.081%; oxygenated product yield, from 3.04%, 3.32%, 3.40% to 4.22%; coke yield, from 1.15%, 1.26%, 1.37% to 1.51%; the alkanes content of liquid products, from 60.03%, 50.60%, 49.71% to 48.15%; the alkenes content of liquid products, from 29.44%, 42.80%, 43.55% to 41.58%. The change of the content of oxygenated compounds content and coke yields is very tiny, and the total content of alkanes and alkenes and the liquid yield of the different times' products have tiny change.

Table-10: The GC-MS analytical result of conversion of oil to bio-fuels under the optimized condition.

No.	RT	Area%	molecular formula	chemical name
1	3.709	3.08	C ₉ H ₂₀	Nonane
2	5.158	3.15	C ₁₀ H ₂₂	Decane
3	6.577	1.5	C ₁₁ H ₂₂	5-Undecene,(E)-
4	6.677	1.8	C ₁₁ H ₂₂	1-Undecene
5	6.709	5.53	C ₁₁ H ₂₄	Undecane
6	6.785	2.75	C ₁₁ H ₂₂	4-Undecene,(E)-
7	6.932	1.54	C ₁₁ H ₂₂	3-Undecene,(E)-
8	8.214	3.29	C ₁₂ H ₂₆	Dodecane
9	9.644	2.49	C ₁₃ H ₂₈	Tridecane
10	10.989	2.86	C ₁₄ H ₃₀	Tetradecane
11	11.658	1.91	C ₁₄ H ₂₈	Cyclopentane,nonyl-
12	12.259	9.67	C ₁₅ H ₃₂	Pentadecane
13	12.934	2.09	C ₁₅ H ₃₀	n-Nonylcyclohexane
14	13.18	2.08	C ₁₅ H ₂₈	Cyclohexene,1-nonyl-
15	13.455	5.5	C ₁₆ H ₃₄	Hexadecane
16	14.027	0.89	C ₁₇ H ₃₆	Tetradecane, 2,6,10-trimethyl-
17	14.228	2.13	C ₁₇ H ₃₄	1-Heptadecene
18	14.359	15.26	C ₁₇ H ₃₄	8-Heptadecene
19	14.594	11.85	C ₁₇ H ₃₆	Heptadecane
20	15.492	2.07	C ₁₈ H ₃₆	5-Octadecene,(E)-
21	15.664	4.66	C ₁₈ H ₃₈	Octadecane
22	16.682	3.13	C ₁₉ H ₄₀	Nonadecane
23	17.661	2.33	C ₂₀ H ₄₂	Eicosane
24	18.445	2.39	C ₂₁ H ₄₂	10-Heneicosene(c,t)
25	18.502	1.28	C ₁₉ H ₃₈ O	9-Octadecene,1-me thoxy-,(E)-
26	18.593	1.77	C ₂₁ H ₄₄	Heneicosane
25	18.668	0.82	C ₁₉ H ₃₈ O	2-Nonadecanone
26	19.166	0.94	C ₁₉ H ₃₆ O	2-Methyl-E,E-3,13- octadecadien-1-ol
27	19.503	0.4	C ₂₂ H ₄₆	Docosane
28	20.047	0.43	C ₂₂ H ₄₆	Heneicosane, 5-methyl-
Total, wt%		99.59		

Table-11: The analytical result of the different liquid products over the 10VNi-10Ce catalyst at the different times.

	the first	the second	the third	the fourth
Liquid yield %	86.68	86.63	86.19	85.90
Gas yield %	11.54	12.05	12.35	12.52
H ₂ O %	0.063	0.068	0.073	0.083
Coke yield %	1.15	1.26	1.38	1.49
Composition of the liquid product				
Cyclic compounds	5.96	6.3	6.54	6.74
alkanes	60.03	45.86	44.66	43.15
alkenes	29.44	43.92	45.16	45.58
Oxygenated compounds	3.04	3.16	3.45	4.22
C ₈ -C ₁₀ wt%	6.43	5.82	6.79	6.46
C ₁₁ -C ₁₈ wt %	75.01	68.85	67.23	67.18
C ₁₈ ⁺ wt %	18.15	24.57	25.79	26.05
Total, wt%	99.59	99.24	99.81	99.69

FT-IR spectra of the different times liquid products over the 10VNi-10Ce catalysts were described and shown in Fig. 10. Compared with FT-IR graph of the crude oil, the intensity of the C=O bond stretch is weak in different times' products. The selective deoxidization on the 10VNi-10Ce catalysts can be done in different times, and the decarboxylation and decarbonylation reaction were excellently fulfilled. The results of BET were analyzed by both the fresh and used catalyst. It can be seen from Table-1, the stability of the catalyst was excellent. The catalyst deactivation was due to coke deposition, relatively to sintering.

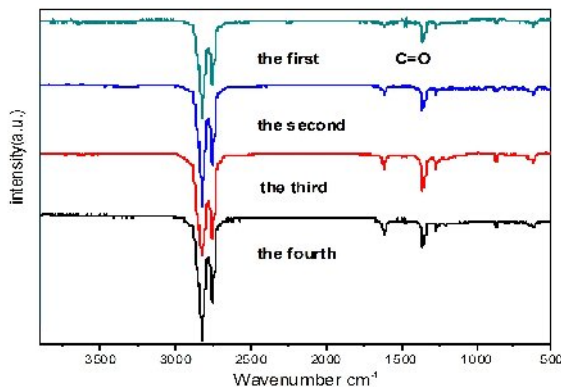


Fig. 10: FT-IR spectra of the different liquid products over the 10VNi-10Ce catalyst at the different times.

The Possible Mechanism and Related Equations

The bond energy of C = O is about 736 ~ 749KJ·mol⁻¹, and the bond energy of C - O bond with 360KJ·mol⁻¹ and the bond energy of C - C with 347KJ·mol⁻¹, so the reaction of C - O and C - C bond breaking is more easy at the beginning of the reaction when the reaction temperature increased, and the

crude oil easily changed into fatty acid and short chain hydrocarbon fracture.

According to the data of GC-MS of the different reaction conditions, the main product is the hydrocarbon compounds under C₁₈. Most alkanes and alkenes are hydrocarbons with C₁₁~C₁₈, moreover, odd carbon hydrocarbons with C₁₅ and C₁₇ are the main compounds. From the results of GC-MS, GC, SF-3 and the FT-IR, we speculate that the first mechanism is one or more fatty acid ester chain γ -H transfer, directly generate less of a carbon atom chain, fatty acid and the unstable intermediate enol. The rapeseed oil changed into fatty acids and other middle products when the reaction temperature increased, and fatty acids partly became alcohol and small quantity of H₂O was produced by dehydration of alcohol. The above interpret is agreed with S. Kovács [34], Katikaneni S. P. R. [38] and Vonghia E. [39]. The related mechanism and equations are listed below.

Decomposition of the triglycerides and the unstable intermediate enol (Scheme 1- 4):

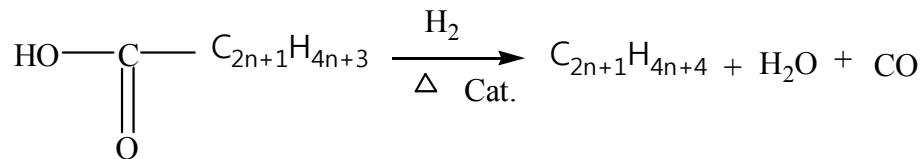
Decarboxylation (-CO₂) and decarbonylation (-CO) reaction of fatty acids:

Decarboxylation and decarbonylation reactions of fatty acids generate odd carbon alkenes and alkanes, and produce CO and CO₂ gas. The proportional relationship of CO and CO₂ is changing with the time and the decarboxylation reaction was the main reaction. In the H₂ condition, odd alkanes and alkenes are the formation of partial olefins by the hydrogenation (Scheme 5- 7):

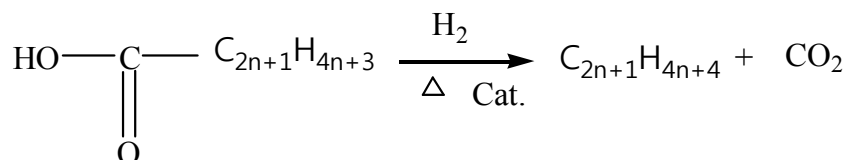
The formation of the even carbon alkanes and alkenes (Scheme 8- 9):

Splitting decomposition of fatty acids and paraffin (Scheme 10- 11):

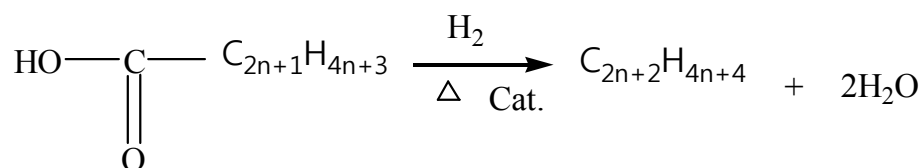
According to the data of GC-MS, the liquid product contains a small amount alkanes and aromatic hydrocarbon and alkenes of C₈~C₁₁. Because the number of carbon atoms of the fatty acid in the crude oil is mainly made of C₁₄, C₁₆, C₁₈, C₂₀ and C₂₂ carbon atoms, alkanes and aromatic hydrocarbon and alkenes of C₈~C₁₁ mostly caused by the common effect of thermal cracking and catalytic cracking.



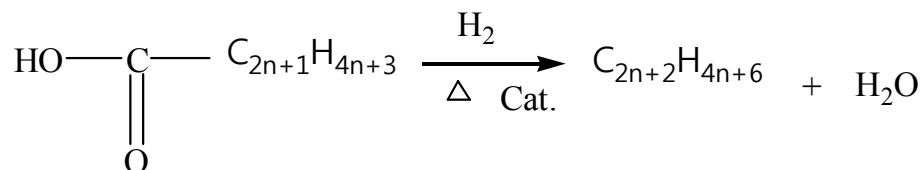
Scheme-6: The formation of odd alkanes.



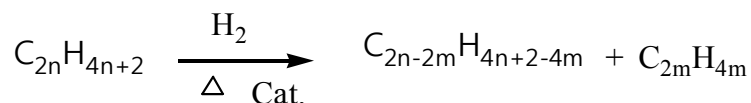
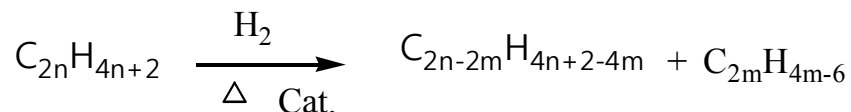
Scheme-7: The formation of odd alkanes.



Scheme-8: The formation of the even carbon alkenes.



Scheme-9: The formation of the even carbon alkanes.

Scheme-10: The formation of C₈~C₁₁ alkanes and alkenes.Scheme-11: The formation of C₈~C₁₁ aromatic hydrocarbon.

Conclusions

The 10VNi-10Ce catalyst has good thermal stability and three kinds of acidity sites on the surface. Compared with sintering, the catalyst deactivation was due to coke deposition. The strong acid site is beneficial to the catalyst activity of the hydrogenation reaction and the deoxidation reaction. The results of FT-IR, SF-3, GC and GC-MS indicate that reaction temperature and oil velocity are

very important factors in producing bio-fuels. The technique was optimized under such circumstances -- reaction temperature at 450°C, reaction pressure at 3.0MPa, oil velocity at 0.1mL/min and the gas velocity at 30mL/min. The alkanes compound content and the alkenes compound content of liquid products are 60.03% and 29.44%, respectively. The main products are the hydrocarbon compounds under C₁₈ and the molar ratio of the diesel oil boiling range target fraction was relatively high (69.04-85.08%).

Most alkanes and alkenes are hydrocarbons with C₁₁~C₁₈, moreover, odd carbon hydrocarbons with C₁₅ and C₁₇ are the main compounds.

The results of GC online and trace water determination indicate that the reaction of decarboxylation and decarbonylation occurred at the same time and the decarboxylation reaction was the main reaction. The most oxygen in the oil were removed by decarboxylation (-CO₂) and decarbonylation (-CO) and the minor oxygen in the oil were removed by the form of H₂O. From the results of FT-IR, SF-3 and GC-MS, researchers deduce the generating mechanism of Non- ester renewable diesel. The research result of continuous conversion of rapeseed oil to bio-fuels provided a theoretical foundation and scientific basis for solving the problems of energy shortage.

Acknowledgements

The authors gratefully acknowledge the financial support of this study by the national natural science foundation china(No.21466021), and the foundation of educational department of Jiangxi Province (No.GJJ11276 and No.GJJ11409), and the important foundation of technological department of Jiangxi Province (No.20111BBF60028) .

References

1. . N. Chheda, G. W. Huber and J. A. Dumesic, Liquid - Phase Catalytic Processing of Biomass-Derived Oxygenated Hydrocarbons to Fuels and Chemicals, *Angew.Chem. Int. Ed.*, **46**, 7164 (2007).
2. V. Bambang, Y. H. Jae, K. K. Seok, S. A. Hong, J. K. Young, S. L. Jong, Y. W. Shu, S. G. Oh and K. Jaehoon, Production of Renewable Diesel by Hydroprocessing of Soybean Oil: Effect of Catalysts, *Fuel*, **94**, 578 (2012).
3. P. Mäki-Arvela, M. Snåre, K. Eränen, J. Myllyoja and D. Y. Murzin, Continuous Decarboxylation of Lauric Acid Over Pd/C Catalyst, *Fuel*, **87**, 3543 (2008).
4. A. A. Martínez, J. S. Luna, J. G. S. Hernandez, S. Hernandez, F. I. G. Castro and A. J.C. Montoya, Dehydration of Bioethanol by Hybrid Process Liquid -Liquid Extraction/Extractive Distillation, *Ind.Eng.Chem.Res.*, **51**, 5847 (2012).
5. R. Nava, B. Pawelec, P. Castaño, M. C. Álvarez Galván, C. V. Loricera and J. L. G. Fierro. Upgrading of Bio-Liquids on Different Mesoporous Silica-Supported Co/Mo catalysts, *Appl. Catal. B-Environ.*, **92**, 154 (2009).
6. J. G. Immer, M. J. Kelly and H. H. Lamb, Catalytic Reaction Pathways in Liquid-Phase Deoxygenation of C₁₈ Free Fatty Acids, *Appl. Catal. A-Gen.*, **375**, 134 (2010).
7. N. J. Luo, K. Ouyang, F. H. Cao and T. C. Xiao, Hydrogen Generation from Liquid Reforming of Glycerin Over Ni-Co Bimetallic Catalyst, *Biomass Bioenergy*, **34**, 489 (2010).
8. M. Watanabe, T. Iida and H. Inomata, Decomposition of a Long Chain Saturated Fatty Acid with Some Additives in Hot Compressed Water, *Energ. Convers Manage.*, **47**, 3344 (2006).
9. D. N. James, J. K. William, A. M. Benjamin and R. C. Ronald, Membrane-Mediated Delivery of Carbon Dioxide for Consumption by Photoautotrophs: Eliminating Thermal Regeneration in Carbon Capture, *Ind.Eng.Chem.Res.*, **51**, 4673 (2012).
10. C. J Chuck, C. D. Bannister, J G. Hawley and M. G Davidson. Spectroscopic Sensor Technique Applicable to Real-Time Biodiesel Determination, *Fuel*, **89** 457 (2010).
11. P. Y. Sun, J. Sun, J. F. Yao, L. X. Zhang and N. P. Xu, Continuous Production of Biodiesel from High Acid Value Oils in Microstructured Reactor by Acid-Catalyzed Reactions, *Chem. Eng. J.*, **162**, 364 (2010).
12. L. X. Li, C. Edward, R. Jeffrey, L. M. Jonathan and W. Devin, Catalytic Hydrothermal Conversion of Triglycerides to Non-ester Biofuels, *Energ. Fuels*, **24**, 1305 (2010).
13. L. C. Meher, D. V. Sagar and S. N. Naik, Technical Aspects of Biodiesel Production by Transesterification-a Review, *Renew. Sust. Energ. Rev.*, **10**, 248 (2006).
14. Q. Shu, B. L. Yang, H. Yuan, S. Qing and G. L. Zhu, Synthesis of Biodiesel from Soybean Oil and Methanol Catalyzed by Zeolite Beta Modified with La³⁺, *Catal. Commun.*, **8**, 2159 (2007).
15. D. N. Sharmila, M. Rosfarizan, A. R. Raha and A. R. J. Nor'Aini, Potential of Bioethanol Production from Nypa Fruticans Sap by a Newly Isolated Yeast *Lachancea fermentati*, *J. Renew. Sustain.Ener.*, **4**, 033110 (2012).
16. H. S. T. Douglas, K. Houssein, K. S. N. Denny, M. E. Mahmoud and R. T. Raymond, Conceptual Synthesis of Gasification-Based Biorefineries Using Thermodynamic Equilibrium Optimization Models, *Ind.Eng.Chem.Res.*, **50**, 10681 (2011).
17. J. M. Marchetti, V. U. Miguel and A. F. Errazu,

- Possible Methods for Biodiesel Production, *Renew. Sust. Energ. Rev.*, **11**, 1300 (2007).
18. Y. Warabi, D. Kusdiana and S. Saka, Reactivity of Triglycerides and Fatty Acids of Rapeseed Oil in Supercritical Alcohols, *Bio-Resource Technol.*, **91**, 283 (2004).
 19. D. Y. Murzin, I. Kubičková, M. Snåre, P. Mäki-Arvela and J. Myllyoja, PCT International Application WO, 075057 A2 (2006).
 20. A. R. Pinho, M. Silva, A. P. S. Neto and J. A. R. Cabral, United States Patent, US, 7540952 B2 (2009).
 21. J. A. Petri and T. L. Marker, United States Patent, US, 7511181 B2 (2009).
 22. D. Y. Murzin, I. Kubičková, M. Snåre, P. Mäki-Arvela and J. Myllyoja, United States Patent, US, 7491858 B2 (2009).
 23. M. X. He, H. Qin, X. B. Yin, Z. Y. Ruan, F. R. Tan, Bo Wu, Zong-xia Shui, Li-chun Dai, Direct Ethanol Production from Dextran Industrial Waste Water by *Zymomonas Mobilis*, *Korean J. Chem. Eng.*, **31**, 2003 (2014).
 24. M. Snåre, I. Kubičková, P. Mäki-Arvela, K. Eranen and D. Y. Murzin, Heterogeneous Catalytic Deoxygenation of Stearic for Production of Biodiesel, *Ind. Eng. Chem. Res.*, **45**, 5708 (2006).
 25. D. Kubička and L. Kaluža, Deoxygenation of Vegetable Oils Over Sulfided Ni, Mo and NiMo Catalysts, *Appl. Catal. A-Gen.*, **372**, 199 (2010).
 26. I. Simakova, O. Simakova, P. Mäki-Arvela, A. Simakov, M. Estrada and D. Y. Murzin, Deoxygenation of Palmitic and Stearic Acid Over Supported Pd Catalysts: Effect of Metal Dispersion, *Appl. Catal. A-Gen.*, **355**, 100 (2009).
 27. M. Snåre, I. Kubičková, P. Mäki-Arvela, D. Chichova, K. Eranen and D. Y. Murzin, Catalytic Deoxygenation of Unsaturated Renewable Feedstocks for Production of Diesel Fuel Hydrocarbons, *Fuel*, **87**, 933 (2008).
 28. I. Kubičková, M. Snåre, K. Eranen, P. Mäki-Arvela and D. Y. Murzin, Hydrocarbons for Diesel Fuel Via Decarboxylation of Vegetable Oils, *Catal. Today*, **106**, 197 (2005).
 29. Y. Takemura, A. Nakamura, H. Taguchi and K. Ouchi, Catalytic Decarboxylation of Benzoic Acid, *Ind. Eng. Chem. Prod. Res. Dev.* **24**, 213 (1985).
 30. P. T. Do, M. Chiappero, L. L. Lobban and D. E. Resasco, Catalytic Deoxygenation of Methyl - Octanoate and Methyl - Stearate on Pt/Al₂O₃, *Catal. Lett.*, **130**, 9 (2009).
 31. S. Lestari, P. Mäki-Arvela, K. Eranen, J. Beltramini, G. Q. Max Lu and D. Y. Murzin, Diesel - like Hydrocarbons from Catalytic Deoxygenation of Stearic Acid over Supported Pd Nanoparticle on SBA-15 Catalysts, *Catal. Lett.*, **134**, 250 (2010).
 32. I. Simakova, O. Simakova, P. Mäki-Arvela and D. Y. Murzin, Decarboxylation of Fatty Acids over Pd Supported on Mesoporous Carbon, *Catal. Today*, **150**, 28 (2010).
 33. O. İ. Şenol, T. R. Viljava and A. O. I. Krause, Hydrodeoxygenation of Methyl Esters on Sulfided NiMo/ γ -Al₂O₃ and CoMo/ γ -Al₂O₃ Catalysts, *Catal. Today*, **100**, 331 (2005).
 34. S. Kovács, T. Kasza, A. Thernesz, I. W. Horváth and J. Hancsok, Fuel Production by Hydrotreating of Triglycerides on NiMo/Al₂O₃/F Catalyst, *Chem. Eng. J.*, **176**, 237 (2011).
 35. I. Baldychev, J. G. Raymond and M. V. John, The Impact of Redox Properties on the Reactivity of V₂O₅/Al₂O₃ Catalysts, *J. Catal.*, **269**, 397 (2010).
 36. A. V. Shijina and N. K. Renuka, Single Step Conversion of Benzene to Phenol Using Hydrogen Peroxide Over Modified V₂O₅/Al₂O₃ Systems, *React. Kinet. Catal. Lett.*, **98**, 139 (2009).
 37. B. Veriansyah, J. Y. Han and S. K. Kim, S. A. Hong, Y. J. Kim, J. S. Lim, Y. W. Shu, S. G. Oh, J. Kim, Production of Renewable Diesel by Hydroprocessing of Soybean Oil: Effect of catalysts, *Fuel*, **94**, 578 (2012).
 38. S. P. R. Katikaneni, J. D. Adjaye and N. N. Bakhshi, Performance of Aluminophosphate Molecular Sieve Catalysts for the Production of Hydrocarbons from Wood-Derived and Vegetable Oils, *Energ. Fuel*, **9**, 1065 (1995).
 39. E. Vonghia, D. G. B. Boocock and S. K. Konar, Pathways for the Deoxygenation of Triglycerides to Aliphatic Hydrocarbons over Activated Alumina, *Energ. Fuel*, **9**, 1090 (1995).